J Biol Inorg Chem (2014) 19:541–554
DOI 10.1007/s00775-013-1080-7

MINIREVIEW

Multicopper oxidases: intramolecular electron transfer and O_2 reduction

Scot Wherland · Ole Farver · Israel Pecht

Received: 16 September 2013 / Accepted: 18 December 2013 / Published online: 16 January 2014

Abstract The multicopper oxidases are an intriguing, widespread family of enzymes that catalyze the reduction of O_2 to water by a variety of single-electron and multiple-electron reducing agents. The structure and properties of the copper binding sites responsible for the latter chemical transformations have been studied for over 40 years and a detailed picture is emerging. This review focuses particularly on the kinetics of internal electron transfer between the type 1 (blue) copper site and the trinuclear center, as well as on the nature of the intermediates formed in the oxygen reduction process.

Keywords Oxidases · Copper proteins · Electron transfer · Metalloprotein · Oxygen

Responsible Editors: Lucia Banci and Claudio Luchinat.

S. Wherland
Department of Chemistry,
Washington State University,
Pullman, WA 99164-4630, USA
e-mail: scot_wherland@wsu.edu

O. Farver
Department of Analytic and Bioinorganic Chemistry,
University of Copenhagen,
2100 Copenhagen Ø, Denmark
e-mail: ole.farver@sund.ku.dk

I. Pecht (✉)
Department of Immunology,
The Weizmann Institute of Science,
76100 Rehovot, Israel
e-mail: israel.pecht@weizmann.ac.il

Introduction

Multicopper oxidases (MCOs) are found throughout the biological domains, with characterized examples from archaea, bacteria, and eukaryotes, including fungi and plants and all the way to mammals. They function by oxidizing, typically by single-electron transfer and with differing specificity [1], a rather wide range of substrates from polyphenols, lignin, and ascorbate to transition metal ions. Concomitantly, O_2 is reduced, producing two water molecules without release of intermediates. Interest in this family of enzymes from the biological inorganic chemistry community has focused particularly on the copper ion binding sites and the mechanisms of electron transfer (ET) and O_2 reduction. The conserved structure of the metal ion sites includes the type 1 (T1) copper ion, with at least two histidine imidazoles and one cysteine thiolate ligand, and a trinuclear center (TNC) comprising a pair of type 3 (T3) copper ions, each coordinated by three histidine imidazole residues, and a type 2 (T2) copper ion coordinated by two histidine imidazoles and usually a water molecule [2]. This review starts with an introduction to the structure of the TNCs as known from X-ray crystallography, followed by a presentation of results, primarily from pulse radiolysis studies, on the intramolecular ET from the T1 site to the TNC in several representatives of the MCO family. This is followed by a discussion of known or proposed O_2 reduction intermediates with an emphasis on the peroxide intermediate, and the overall mechanism.

Structure of the TNC in MCOs

MCOs are typically composed of a single polypeptide chain with three cupredoxin-structured domains, but there

are also enzymes with only two domains that exist as trimers [3–6], illustrated by the small laccase (SLAC) from *Streptomyces coelicolor* [3, 4]. Ceruloplasmin is another variant with six domains in a single chain [7]. These variations have led to analysis of the evolutionary relationships among the enzyme sequences derived from the organisms producing the different variants [5, 6, 8, 9].

The plethora of available 3D structures of MCOs determined by X-ray crystallography, some at a resolution better than 2.0 Å, represent enzymes from divergent sources and exposed to different conditions of O_2 and reducing substrates which provide interesting and important insights into the evolution of this family and should similarly help in the understanding of the O_2 reduction mechanism. Unfortunately, the picture that has so far emerged from the 3D structures is not as clear as was hoped, a situation that can be traced to several causes:

1. The structures include at least 500 residues and thus are moderately large structures to solve and high resolution is required to delineate the small but critical changes in O–O, Cu–Cu, and Cu–ligand bond lengths and angles often relevant to distinguishing mechanistic alternatives.
2. Several structures lack a full complement of copper ions (especially T2).
3. Different constraints have been applied on certain bond lengths during crystallographic refinement.
4. Most significantly, strongly reducing radicals, produced by the radiolysis of water by X-rays, lead to the progressive reduction of the Cu(II) sites. This is especially an issue since structures are now routinely obtained using high-intensity synchrotron sources. The 3D structure of the T1 site hardly varies with the change in the copper oxidation state, whereas that of the TNC is expected to change significantly, particularly due to interaction with O_2 and its reduction intermediates.
5. Progressive reduction of the protein induced by X-rays will lead to different structures at some of the otherwise crystallographically identical sites, resulting in the averaging of structures in the refinement.
6. Atomic motions that might normally accompany reduction of the enzyme are likely to be restricted by the protein itself, especially under the low-temperature conditions typical for these experiments, and thereby possibly leading to nonequilibrium structures.

Thus, the structure of a protein that is reduced after it has been crystallized, either by soaking with a reducing agent or by irradiation at low temperatures, may not be the same as if it were crystallized in the reduced state. In contrast, when crystals are exposed to reducing agents at room temperature, the metal centers may relax to the functionally relevant structures as elegantly illustrated by Liu et al. [10]. A further example of the need for caution is the refinement of the structure of the laccase from the spore coat protein of *Bacillis subtilis* (CotA) [11], which initially showed O_2 in the substrate channel, but in the most recent refined structure the position was altered to a more typical location between the T3 copper ions (Protein Data Bank code 3ZDW replacing 1UVW).

These cautions notwithstanding, there is much that can be learned from selected studies, especially when trends can be found within a series of structures. A particularly careful and instructive study is that of the laccase from the fungus *Steccherinum ochraceum*, in which multiple crystals were used to collect X-ray data at differing radiation doses (Protein Data Bank codes 3T6W, 3T6X, 3T6Z, 3T71) but at the same resolution of 2.15 Å. This study also used crystals grown at pH 9.0 in an attempt to slow the proton transfers occurring in the final steps of O_2 reduction [12]. The result was a series of structures, each with three independent TNC sites, that can be used as the basis for a discussion of the mechanism. The structure that absorbed the lowest radiation dose and was partially reduced (10 % of the dose required to fully reduce the protein, but enough to reduce 50 % of the T1 copper ions) has two TNC sites, in each of which an O_2 molecule is asymmetrically bound outside the TNC and there is a water molecule or hydroxide ion within the cluster and bridging the T2 copper ion and one of the T3 copper ions. The T3 copper ions are separated by 3.7 Å. These structures are the closest examples to an oxidized site from this series. The same, lowest-dose, structure also exhibits one TNC with O_2 symmetrically bound, having equal distances between the T3 copper ions and both oxygen atoms, and having a T3 Cu–Cu separation of 3.8 Å, while the O–O distance is the same as that of an oxygen double bond, 1.2 Å. This structure may represent the initial step of the mechanism, O_2 binding to presumably reduced T3 copper ions. Structures showing further extents of reduction will be discussed in the section "O_2 reduction mechanism and intermediates." Most significantly for consideration of T1 copper to TNC ET, there is no change in the dimensions of the T1 site, or in the distance between the T1 and T3 copper atoms. The pioneering determination of an MCO structure, which also provided decisive insights into functional features of MCOs, was that of ascorbate oxidase (AO) from zucchini (*Cucurbita pepo medullosa*) in both oxidized [13, 14] and reduced [15] states. Further, it had the advantage of being determined without use of synchrotron radiation. Here the T3 Cu–Cu distance is 5.1 Å in the reduced state produced by soaking the crystal in dithionite solution, showing only a distant nonbridging oxygen present in most structures [15]. The long Cu–Cu distance is most similar to that observed for the *S. ochraceum* laccase after absorption of the largest radiation dose (vide infra).

Intramolecular ET in MCOs

The structure of MCOs has apparently been evolutionarily optimized for reduction of O_2, involving intramolecular single-electron transfer from the electron uptake site, T1 Cu(II), to the TNC in the catalytic reduction half-cycle. The T1 Cu(II) ion serves as the site for electron uptake from rather diverse substrates, whereas O_2 undergoes four-electron reduction to two water molecules at the TNC. The T1 site is near the enzyme surface and is connected to the TNC by a covalent linkage as described below. The electronic characteristics of the T1 Cu(II) center are mainly due to the highly efficient charge transfer due to mixing of the $S_{p\pi}$ and Cu $3d_{x^2-y^2}$ orbitals and the distorted tetrahedral geometry. The resulting highly covalent Cu–S bond gives rise to a large degree of anisotropic covalency that dominates the properties of the MCOs. This, together with the rather limited changes in the T1 copper geometry accompanying the redox change, minimizes the reorganization requirement of the ligand sphere [16]. Although the T1 copper coordination sphere is essentially conserved throughout all the structures determined, variability is observed in the nearby surface residues that form the binding sites that accommodate different electron-donating substrates. The TNC interacts with the oxidizing substrate O_2, but the bonds with it and with the intermediates formed in the reduction process may change. This raises several important questions:

1. Does the internal T1 copper to T3 copper ET rate depend on the number of reduction equivalents taken up by the enzyme?
2. What structural changes is the TNC undergoing during reduction, and how do these affect the internal ET rate?
3. How does the presence of O_2 affect the internal ET rates (i.e., by enhancing the driving force or additionally by an allosteric mechanism [17])?
4. Which intermediates are formed during the catalytic reduction of O_2 and how do these depend on the degree of the enzyme's reduction?
5. Is the enzyme, as isolated, fully active or must it be activated to achieve maximal catalytic efficiency?

The 3D structures of AO in both oxidation states as well as those of its complexes with azide and peroxide [13, 14, 18] provided the first structural proposal for covalent ET pathways from T1 Cu(I) to T3 Cu(II) (a through-space separation of either 12.2 or 12.6 Å) in MCOs. The paths proceed through 11 covalent bonds from the T1 copper, via the Cys507 thiolate ligand (S_γ) to the imidazole (N_ε) of either His506 or His508 to each T3 copper ion [13, 19] (Fig. 1). As mentioned above, the anisotropic thiolate–copper covalency enhances the electronic coupling between both Cu(II) and Cu(I) with Cys-(S_γ).

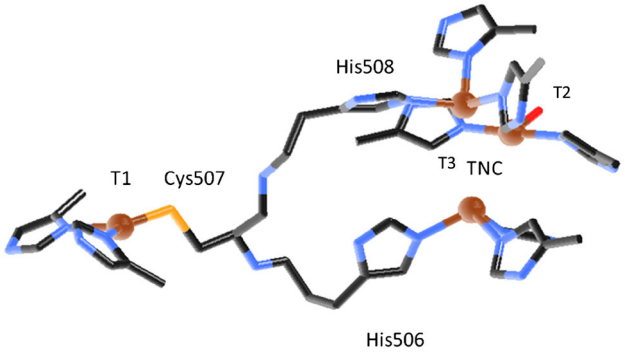

Fig. 1 Intramolecular electron transfer (ET) pathway from type 1 (*T1*) Cu(I) to the trinuclear center (*TNC*) [type 2 (*T2*) copper and type 3 (*T3*) copper] in *Cucurbita pepo medullosa* ascorbate oxidase (AO). The two covalent paths connecting Sγ of Cys507, the ligand of the T1 copper ion, and the Nε of His506 and His508, ligands of the T3 copper ions, are shown. The direct T1 copper to T3 copper distance is 11.8 Å. The coordinates were taken from the Protein Data Bank (code 1AOZ [13])

The internal ET process between the T1 site and the TNC has been studied, mainly by fast reaction techniques such as pulse radiolysis, laser flash photolysis [20], and rapid-freeze EPR [21]. When experiments using the pulse radiolysis and flash photolysis methods were performed in the absence of oxygen, the net reduction process of the enzymes could be examined. Both these methods make possible measurements of fast reaction steps, providing different electron donors or acceptors produced by either the radiation or light pulses, down to at least the submicrosecond domain. Whereas the former method requires use of specific reagents that allow conversion of the reactive and nonselective primary radicals produced by the radiation, the latter method involves the use of chromophores that are usually the actual electron donor to the enzyme examined. Pulse radiolysis studies have clearly established that the electron uptake site of MCOs is the T1 Cu(II), and this is followed by slower internal ET to the T3 site. Significantly, monitoring the time course of absorbance changes at both approximately 600 nm (T1 site) and approximately 330 nm (T3 site or TNC) along with concentration independence of the rate demonstrated that this is an internal single-electron transfer process.

ET theory

In the nonadiabatic regime, the semiclassical ET theory for reactions between spatially fixed and oriented donors and acceptors provides a framework for analysis of rate constants [22]:

$$k_{ET} = \sqrt{\frac{4\pi^3}{h^2 \lambda_{TOT} k_B T}} H_{DA}^2 \exp\left\{ -\frac{(\Delta G^0 + \lambda_{TOT})^2}{4\lambda_{TOT} k_B T} \right\}, \quad (1)$$

where h is Planck's constant, k_B is Boltzmann's constant, T is the temperature (K), H_{DA} is the electronic coupling between the electron donor and electron acceptor through the ET pathway, $-\Delta G^0$ is the driving force for the ET, and λ_{TOT} is the free energy of reorganization, a measure of the overall change in bond lengths and angles as a result of the redox changes. It is important to stress that the total reorganization energy includes terms from both the inner-sphere reorganization of the copper center and its ligands, and the reorganization of the environment, including neighboring residues and solvent. When the driving force of the reaction equals the total reorganization energy, the rate constant reaches its maximum value, k_{MAX}. ${H_{DA}}^2$ decays exponentially with the separation distance, and we may estimate the pre-exponential factor in Eq. 1 as k_{MAX} in Eq. 2:

$$k_{MAX} = \frac{k_B T}{h} \exp[-\beta(r - r_0)], \quad (2)$$

where r is the donor–acceptor distance and r_0 is the value of r for a donor and an acceptor in direct (van der Waals) contact. The electronic decay factor, β, is estimated to be approximately 10 nm^{-1} in proteins [23].

In the following, a few specific examples of results of studies of the internal T1 copper to T3 copper ET reaction will be described.

Trametes hirsuta laccase

Intramolecular ET in *T. hirsuta* laccase was studied [24], and Fig. 2a illustrates the biphasic process monitored at 610 nm. The bimolecular reduction of T1 Cu(II) by pulse-radiolytically produced ${CO_2}^-$ radicals is followed by a slower, unimolecular reoxidation of T1 Cu(I). Reduction of T3 Cu(II) was observed in the slower time domain (Fig. 2b) with an essentially identical, concentration-independent rate constant ($k_{ET} = 25\ s^{-1}$ at 298 K; Table 1) and this reaction step is assigned to an intramolecular T1 Cu(I) to T3 Cu(II) equilibration:

$$T1[Cu(I)]T2/T3[Cu(II)] \leftrightarrows T1[Cu(II)]T2/T3[Cu(I)]. \quad (3)$$

Since Eq. 3 represents an equilibrium, k_{ET} is the sum of rate constants for forward (k_f) and backward (k_b) reaction steps; i.e., $k_f/k_b = K$. From the amplitudes of the absorption changes of the T1 copper and T3 copper bands, the latter equilibrium constant K can be determined and hence so can the individual rate constants. During the stepwise reductive titration of the enzyme caused by introduction of sequential pulses, the T1 Cu(I) is only partially reoxidized, and from the electron equilibration with the T3 site, $K = 0.4$ was determined at 298 K. This corresponds to a reduction potential difference of 24 mV between the T1 and T3 sites. It is noteworthy that no further reduction of the T1 copper site is observed beyond uptake of 2.9 ± 0.2 electron equivalents by the enzyme. Thus, only three of the four redox centers are apparently reduced. The reduction potential of the T2 Cu(II)/(I) center in *T. hirsuta* laccase has been determined to be approximately 400 mV at pH 6.5 [29], close to the potential of the analogous *Trametes versicolor* laccase of 405 mV [30], which is significantly lower than for the other copper sites ($E^0_{T1} = 780$ mV; $E^0_{T3} = 756$ mV) [24], indicating that there is not sufficient driving force for T3 copper to T2 copper ET. Thus, 56 % reduction of T1 copper, 44 % of T3 copper and practically no reduction of T2 copper were observed [24]. Following the uptake of three electron equivalents, the T1 and T3 copper ions are reduced and no further electrons are taken up by the *T. hirsuta* laccase. It is noteworthy that the absorbance decay of the 330-nm band occurs after one-electron reduction of an enzyme molecule and synchronously with an increase in absorption of T1 Cu(II) [31]. This implies that uptake of a single electron equivalent by the TNC suffices to cause complete loss of its 330-nm band. This conclusion is reached by accurate evaluation of the amplitudes of the internal ET process: the amplitude of the absorption increase due to T1 Cu(I) reoxidation and the decrease at 330 nm caused by its reduction are equivalent on the basis of the respective extinction coefficients of the two bands (see Fig. 2).

Rhus vernicifera laccase

The first kinetic study resolving the intramolecular ET in a blue MCO was performed on *R. vernicifera* laccase [24, 25]. A rather slow rate of 1.1 s^{-1} at pH 7.0 and 298 K was determined for the T1 copper and T3 copper electron equilibration, monitored at both 625 nm [T1 Cu(II)] and 330 nm [T3 Cu(II)]. As no 3D structural information was available at that time, no further interpretation could be pursued. Later studies [24] confirmed that an intramolecular T1 Cu(I) to T3 Cu(II) ET equilibration occurs as described by Eq. 3. From the amplitudes of T1 copper reduction and reoxidation, an equilibrium constant of 1.5 at 298 K was calculated. The reduction potentials of the copper sites of *R. vernicifera* laccase are 394 mV for the T1 site, 365 mV for the T2 site, and 434 mV for the T3 site, all versus the standard hydrogen electrode at pH 7.5 and 298 K [32]. In line with these data, all three copper sites of the TNC (four electron equivalents, including the T1 site) could be reduced by pulse radiolysis, as has indeed been observed experimentally.

A more than 20-fold increase in the T1 copper to T3 copper ET rate constants was observed between *T. hirsuta* and *R. vernicifera* laccases: 25 s^{-1} (*T. hirsuta* laccase)

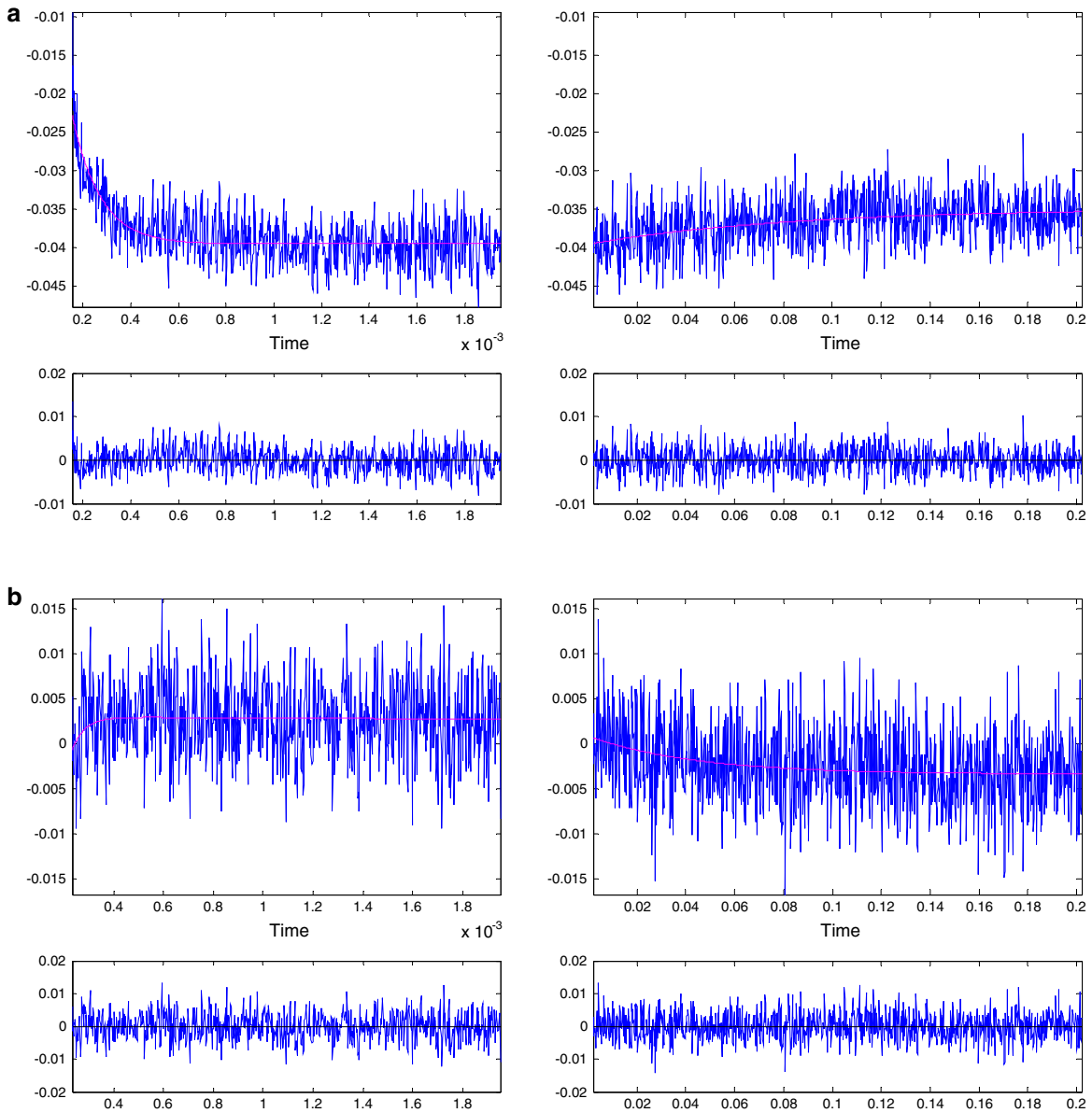

Fig. 2 **a** Time-resolved absorption changes monitored at 610 nm of a 94.5 μM *Trametes hirsuta* laccase solution following pulse radiolysis in N_2O-saturated 100 mM formate, 10 mM phosphate, pH 4.5. Pulse width 0.4 μs, $T = 299$ K. Two time domains were shown; both are in seconds. The *lower frames* show the residuals of the fitted curves. **b** Same process as for **a** monitored at 330 nm. All other conditions are as for **a**. The absorbance changes in the slow phases at 610 and 330 nm agree, further confirming the process is intramolecular ET from T1 Cu(I) to T3 Cu(II). Two time domains are shown; both are in seconds. The lower frames show the residuals of the fitted curves. (From [24])

versus 1 s^{-1} (*R. vernicifera* laccase). In a recent study, catalytic constants were reported for *R. vernicifera* and *T. hirsuta* laccases derived from electrochemical studies using various substrates [33]. The minimum difference in the catalytic constants was for 2, 2′-azinobis(3-ethylbenzothiazoline-6-sulfonic acid; k_{cat} for *T. hirsuta* laccase (196 s^{-1}) was markedly higher than k_{cat} for *R. vernicifera* laccase (10.1 s^{-1}), which is in agreement with the above rate constant ratio for intramolecular ET. It is noteworthy that the steady-state rates are tenfold faster than those of the intramolecular ET calculated from the pulse radiolysis studies in the absence of oxygen. However, O_2 binding to the TNC is expected to markedly increase the driving force; e.g., even a low O_2 concentration increased the rate of intramolecular T1 Cu(I) to T3 Cu(II) ET in AO by a factor of 5 (see later) [28].

Ceruloplasmin

Ceruloplasmin, a mammalian ferroxidase, stands out in the family of MCOs by having a significantly different structure, with six cupredoxin domains in a single polypeptide chain [7]. In addition, it contains three T1 copper sites along with a single TNC associated with one of the T1 copper sites. Pulse radiolysis studies using both hydrated electrons [34] and CO_2^- radicals [26] resolved an initial reduction of apparently exposed disulfide residues to yield $RSSR^-$ radicals that decayed by intramolecular ET ($28 \pm 2\ s^{-1}$ at 279 K) to the T1 centers. By independent monitoring of both the T1 center and the T3 center absorbance changes, a subsequent internal ET between the T1 center and the TNC was observed with a rate constant of $2.9 \pm 0.6\ s^{-1}$. The internal equilibrium constant between the T1 and T3 centers was established as 0.17 (Table 1).

S. coelicolor laccase (SLAC)

Recently a bacterial, two-domain laccase (SLAC) was isolated from *S. coelicolor* [35]. Spectroscopic properties and the 3D structure established the trimeric quaternary arrangement. The intramolecular ET between the T1 and T3 sites was studied by pulse radiolysis [3], and a novel behavior was found: when the enzyme was gradually reduced by introduction of sequential pulses, the intramolecular ET rate constant increased more than tenfold ($15–186\ s^{-1}$). Figure 3 illustrates the observed, slightly sigmoidal increase in the rate constant as a function of the extent of enzyme reduction. Significantly, after the uptake of two electron equivalents, no further ET equilibration occurs, suggesting that a fully reduced T3 site is attained at this stage but also that the T2 Cu(II) is not involved in the equilibration process, in analogy to the behavior observed for the *T. hirsuta* laccase described earlier and reflecting the lower reduction potential of the T2 site . Another feature, resolved in comparing fresh ("as isolated") SLAC solutions and samples reoxidized by O_2 after full reduction by the radicals or by ascorbate ("cycled"), was a marked rate enhancement observed for the "cycled" samples ($8–15\ s^{-1}$).

Activation parameters were derived from temperature dependence measurements of the internal ET rates at different states of SLAC activation and reduction (Table 1). The following reaction mechanism, independent of the enzyme form, was proposed:

$$R^* + T1^{O}T3^{OO} \rightarrow T1^{R}T3^{OO} \leftrightarrows T1^{O}T3^{RO} \quad \text{(internal ET with initial rate)}, \tag{4}$$

$$R^* + T1^{O}T3^{RO} \rightarrow T1^{R}T3^{RO} \leftrightarrows T1^{O}T3^{RR} \quad \text{(internal ET with a higher rate)}, \tag{5}$$

$$R^* + T1^{O}T3^{RR} \rightarrow T1^{R}T3^{RR}, \tag{6}$$

(R^* symbolizes reducing radicals, and the O and R superscripts indicate oxidized and reduced copper centers, respectively).

The marked ET rate enhancement induced on reduction could be caused by changes in electron tunneling pathways, in the driving force, and/or in the reorganization energy [3]. As in other MCOs, the T1 copper ion and the two T3 copper ions are linked by 11 covalent bonds, and the separations are 12.2 and 12.7 Å, respectively [4]. Using an electronic decay factor [23] of $10\ nm^{-1}$ yields $k_{max} = 2.4 \times 10^7\ s^{-1}$; see Eq. 2). The rate constant for the

Table 1 Intramolecular electron transfer (ET) in multicopper oxidases at 298 K

Organism/enzyme	PDB codes	Rate constant (s^{-1})	$\Delta H^{\ddagger}$ (kJ mol^{-1})	$\Delta S^{\ddagger}$ (J mol^{-1} K^{-1})	K	References
Trametes hirsuta laccase	3FPX	25 ± 1	30.7 ± 5.0	-87 ± 9	0.4	[24]
Rhus vernicifera laccase		1.1 ± 0.1	9.8 ± 0.2	-211 ± 3	1.5	[24, 25]
Human ceruloplasmin	2J5W, 1KCW, 2BHF	2.9 ± 0.6 (279 K)			0.17	[26]
Cucurbita pepo ascorbate oxidase (no O_2 present)	1AOZ, 1ASO, 1ASP, 1ASQ	201 ± 8	9.1 ± 1.1	-170 ± 9	1.8	[27]
		2.3 ± 0.2	6.8 ± 1.0	-215 ± 16		
Cucurbita pepo ascorbate oxidase with O_2		$1{,}100 \pm 300$				[28]
Streptomyces coelicolor laccase (SLAC)	3CG8	8 ± 1	25.2 ± 3.2	-142 ± 15	0.4	[3]
		15 ± 3	9.5 ± 3.7	-189 ± 46	5.0	
		186 ± 25	26.2 ± 6.0	-114 ± 18		

The two rate constants for ascorbate oxidase represent two different, simultaneous intramolecular ET processes. The three rate constants for the small laccase (SLAC) from *S. coelicolor* represent different stages of the ET process. The first is the rate constant observed in the "as isolated" protein; the second is that observed after recycling; and the last one is the rate constant after introduction of a series of sequential pulses (see Fig. 3). K is the type 1 copper/type 3 copper equilibrium constant as determined from the pulse radiolysis amplitudes

PDB Protein Data Bank

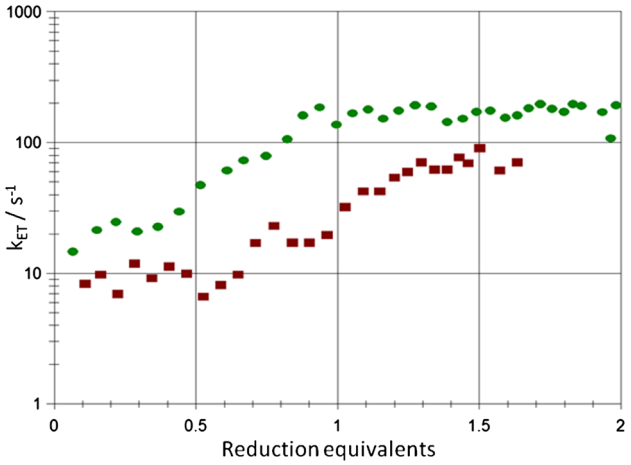

Fig. 3 Observed rate constants of intramolecular T1 Cu(I) to T3 Cu(II) ET in the small laccase isolated from *Streptomyces coelicolor* as a function of sequentially introducing reduction equivalents (25 pulses, 0.3 μs each). *Red squares* 22.7 μM "as isolated" laccase, *green circles* the same solution after being "cycled"; 5 mM 1-methyl nicotinamide, 100 mM *tert*-butanol, 10 mM potassium phosphate, pH 7.3, and 298 K. Argon saturated. (From [3])

initial reduction phase of the "as isolated" enzyme, 8 s^{-1}, corresponds to an activation free energy, $\Delta G^{\ddagger}$, of 0.378 eV. The equilibrium constant for the reaction in Eq. 4 is 0.41 at 298 K, equivalent to a driving force, $-\Delta G^0$, of −0.023 eV. By application of the semiclassical Marcus theory [22] (Eq. 1), a reorganization energy, λ_{TOT}, of 1.46 eV was calculated, which is in good agreement with all previously reported values [36]. The equilibrium constant for the reaction in Eq. 5 is 5.0 (or $-\Delta G^0 =$ 0.041 eV). Thus, the larger driving force contributes slightly to a rate increase, but since $|\Delta G^0| \ll \lambda_{TOT}$, the increase in the ET rate is dominated by changes in the reorganization energy. An approximately 20-fold increase in the rate constant requires a decrease in $\Delta G^{\ddagger}$ to 0.32 eV, which, in turn would require a small (0.2 eV) decrease in λ_{TOT} to 1.3 eV. Thus, the primary cause for the lowering of2 the reorganization energy on partial T3 site reduction could be structural changes either in the coordination sphere of the metal ions or indirectly in the trimeric SLAC quaternary structure, or in both. A semireduced T3 center is a necessary transient species since monitoring the time course of the ET from the T1 site to the binuclear T3 site by means of the 330 and 605 nm bands shows that it proceeds in single-electron transfer steps. As discussed already, on the basis of the available crystal structures, significant structural changes involving the distance between the T3 copper ions and any associated bridging oxygen atoms are expected. The first T1 site to T3 site ET in SLAC probably leads to uncoupling of the T3 copper pair and breaking of the linking OH^- bridge, but does not affect the ET pathway. The structure of a semireduced intermediate would thus be closer to that of the fully reduced state than to that of the oxidized state, and would cause the decrease in λ_{TOT} for the second internal ET step.

Dependence of the intramolecular ET rates on the extent of reduction has so far not been observed in other MCOs (see earlier). However, unlike other monomeric MCOs examined, SLAC is trimeric, and changes in its T3 site coordination sphere may not be the only cause for the enhanced reactivity on reduction. Namely, since the TNC in SLAC is located at a monomer–monomer interface and each T3 copper is bound to ligands from two different monomer chains [3], changes in the TNC reduction state and coordination could also affect the quaternary structure of the trimer and thus provide a structural rationale for the behavior of SLAC, as opposed to AO, *T. hirsuta*, and *R. vernicifera* laccases. Significantly, in the analogous copper nitrite reductases, which are also homotrimers, evidence has indeed been provided for marked interactions among the monomers [6, 37].

Control of internal ET rates by site–site interactions is an intriguing functional feature encountered for the first time in MCOs. An enhanced ET reactivity with increasing extent of reduction and the resultant preference for fully reduced T3 site in SLAC has consequences for the O_2 reduction process. Binding of O_2 to $T1^RT3^{RR}$ or $T1^OT3^{RR}$ would yield a peroxide intermediate (vide infra) promoting additional electron uptake by the enzyme before the crucial steps of O_2 bond splitting and further reduction [38]. This would also be the case in other MCOs where the three-electron-reduced state is prevalent owing to the low redox potential of the T2 Cu(II) and could also reflect preference for the formation of the fully reduced T3 site over two half-reduced ones due to an evolutionary advantage under conditions of limited reducing substrate.

C. pepo medullosa AO

Internal T1 copper to T3 copper ET has been studied by both pulse radiolysis [27, 39] and flash photolysis [20] in *C. pepo medullosa* AO. Interestingly, the two independent pulse radiolysis studies observed multiple phases in the T1 copper to T3 copper ET process (201 ± 8 and 2.3 ± 0.2 s^{-1}; Table 1) from the beginning of the reductive titration. These multiple phases were tentatively attributed to subpopulations of molecules with different TNC structures, especially with respect to bridging or T2 copper coordinated water molecules [27]. A later study [28] was performed using a slight stoichiometric excess of O_2 at the beginning of the pulse radiolysis reductive titration (see Fig. 4). In this case the faster internal ET rate increased to 1,100 ± 300 s^{-1}, but was still below the turnover rate of the enzyme of approximately 12,000 s^{-1} [40], consistent with having the TNC state dependent on

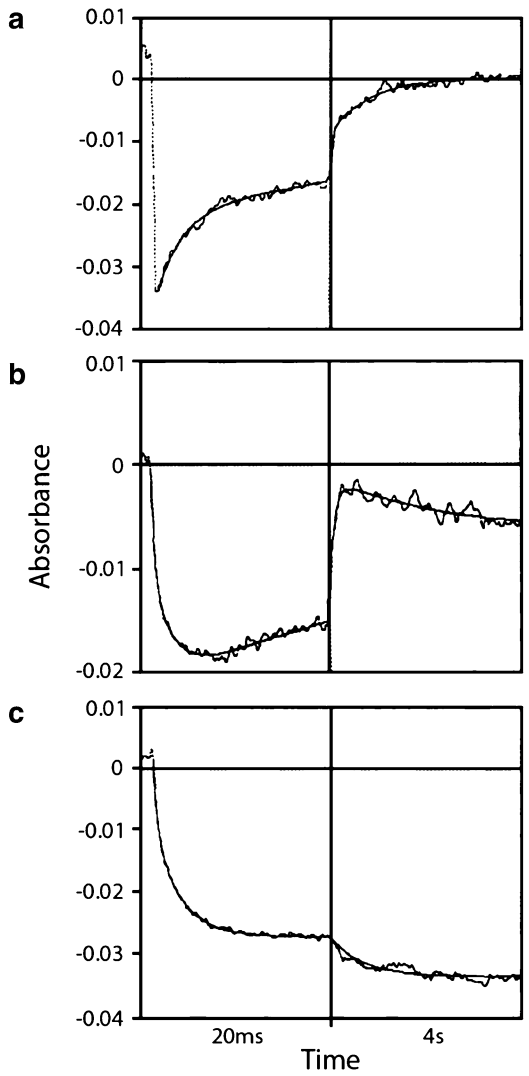

Fig. 4 Time-resolved absorption changes in *C. pepo medullosa* AO. **a** Fast bimolecular reduction of T1 Cu(II) (610 nm) by CO_2^- is followed by intramolecular reoxidation. The conditions were as follows: 5.3 μM AO; 65 μM initial O_2 concentration; pH, 5.8; temperature, 293 K; pulse width, 0.5 μs. **b** Reduction of T3 Cu(II) (330 nm) by intramolecular ET from T1 Cu(I). After intramolecular ET from T1 Cu(I), a net transient increase in the 330-nm (T3 copper) absorption is observed, assigned to formation of AO–O_2 intermediates. The conditions were the same as for **a**. **c** T3 Cu(II) (330 nm) reduction by intramolecular ET from T1 Cu(I) after apparent O_2, exhaustion. The other conditions are as for **a**. (Adapted from [28])

whether it recently underwent a cycle of reduction and reoxidation by O_2 (i.e., being in the "as isolated" or the activated, "pulsed" state). Other important factors could be the availability of higher concentrations of O_2 under physiological conditions, or excess reducing substrate. K_M for ascorbate is 1.4 mM [41]. Under pulse radiolysis conditions, however, there is a large excess of enzyme over reducing radicals; hence, there is not sufficient reductant to maintain the fully reduced state of the enzyme. Although the presence of small amounts of O_2 increases the rate of intramolecular ET considerably, under optimal conditions the concentration of ascorbate is sufficient to maintain a steady state of Cu(I) centers so that turnover is monitored between practically fully reduced AO molecules and O_2.

O_2 reduction mechanism and intermediates

As stated earlier, a major motivation for the broad and intense interest in the structure and reaction mechanism of MCOs is their capacity to efficiently catalyze the four-electron reduction of O_2 to water while overcoming the relatively high energy barriers for reduction of O_2 by one and three electrons, and without release of intermediates, particularly reactive oxygen species. O_2 is kinetically inert to reduction because of two important factors: one-electron reduction of O_2 is thermodynamically strongly unfavorable, and two-electron reduction of O_2 ($S = 1$) to peroxide by organic substrates ($S = 0$) is spin-forbidden. MCOs catalyze the four-electron reduction of O_2 to two water molecules by providing the necessary thermodynamic driving force for either two sequential two-electron steps or first by a concomitant two-electron reduction of O_2 to form a TNC-bound peroxide followed by two single-electron transfers, combined with H^+ transfer from protein amino acid side chains or coordinated water molecules (see below) [42–45]. Two carboxylates are generally conserved [44]: specifically, Glu498 and Asp116 of CotA have been demonstrated to be involved, as have Glu506 and Asp112 in the *Escherichia coli* MCO CueO. In both reductions, the highly endergonic step of superoxide formation is circumvented.

The last four decades has provided a very large amount of biochemical, structural, spectroscopic, and kinetic information, yet detailed models of the reaction mechanisms are still not fully established [46–48]. One important reason for this situation is the known structural differences among MCO subfamilies that may lead to differences in their mechanism of O_2 reduction. Attention to this possibility has been raised only recently [49].

Studies of the reductive half-cycle of MCOs have focused on ET kinetics using diverse physiological and nonphysiological substrates. There is general agreement that the T1 Cu(II) is the electron uptake site of all the MCOs characterized. The substrate specificity of many MCOs is relatively broad, but in some cases the 3D structure has suggested specificity, as, for example, for Fe(II) of the ferroxidases, ceruloplasmin, and its analogue Fet3p [50]. The main challenge in understanding the subsequent steps of catalysis is the resolution of the electron distribution between T1 Cu(I) and the components of the TNC and the time courses, first in the absence of O_2 and

then for the individual O_2 reduction intermediates [38, 51–58]. A wide range of experimental and theoretical approaches have been used in efforts to identify such intermediates [46]. One obvious protocol pursued is to study the reaction of the fully reduced enzyme with O_2, whereas other protocols tried dissecting the oxidative half-cycle at different states of O_2 reduction. This is essential in view of the fact that MCOs function under diverse conditions of reducing substrate and O_2 availability. Fast reaction kinetics, monitoring different spectroscopic probes, and oxygen isotopes have helped in identifying or suggesting intermediates [53, 59]. Modified or mutated MCOs, notably those where the T1 copper has been replaced by mercury or depleted, or the T2 copper had been depleted, have also been used to arrest the overall reaction and stabilize intermediates. Since these enzyme forms are devoid of enzymatic activity [60–62], the extent to which the mechanism has been altered remains an open issue.

The most extensively studied intermediate is the MCO-bound peroxide. Pioneering detailed quantitative analyses of the *R. vernicifera* laccase spectra of this species revealed a characteristic optical absorption feature at 325 nm accompanied by a large negative Cotton effect at the same wavelength in the circular dichroism spectra [56]. Moreover, it was shown that the peroxylaccase can be formed in several different and independent ways: by reaction of partially or fully reduced laccase with O_2 (Fig. 5a) [38], by limited reduction of the enzyme in the presence of oxygen, and most importantly, by reacting fully oxidized laccase with 1 equiv of hydrogen peroxide (Fig. 5b) [56, 58]. Some time after these results has been published, the argument was made that the observed spectral features at 325 nm are caused by oxidation of partly reduced T3 sites in the resting laccase rather than by formation of a peroxylaccase [63]. However, this argument can clearly be refuted by several different sets of results showing that the spectral changes are specific to the reaction caused by addition of hydrogen peroxide to laccase, already established to be fully oxidized [38, 56]. Furthermore, neither different strong inorganic one-electron oxidants nor organic two-electron oxidants could produce the above-mentioned specific spectroscopic changes. In addition, measurements of the magnetic susceptibility demonstrated that the electronic coupling between the two T3 Cu(II) ions weakens on coordination of the peroxide group [64]. Last but not least, the quantitative analysis of the reductive titrations of peroxylaccase established that six reduction equivalents are required in order to fully reduce this peroxylaccase derivative (Fig. 6a). Taken together these results are consistent only with the observation of a genuine peroxylaccase formation with a relatively long lifetime and a high affinity, $K \sim 10^9\ M^{-1}$ (Fig. 6b) [55]. Remarkably, the same group challenging the observed

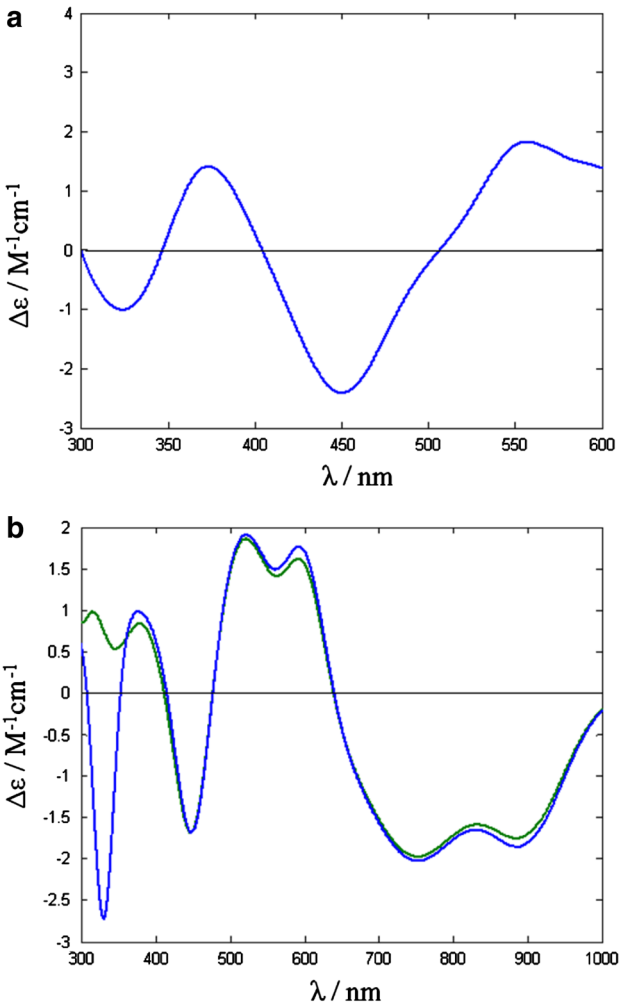

Fig. 5 **a** Circular dichroism spectrum of partly reduced *Rhus vernicifera* laccase reacted with O_2. *R. vernicifera* laccase, 0.09 mM, in 0.1 M phosphate, pH 7.0, 298 K, was reduced with 0.05 mM ascorbate (argon saturated) followed by reoxidation with O_2 [38]. **b** *Blue line* circular dichroism spectrum of peroxylaccase produced by adding 1 molar equivalent of H_2O_2 to *R. vernicifera* laccase, 0.12 mM in 0.1 M phosphate, pH 7.0. *Green line* the same *R. vernicifera* laccase solution before addition of hydrogen peroxide [56]

peroxylaccase formation described above soon afterwards reported that a peroxide is indeed produced as an intermediate in the course of O_2 reduction by fully reduced laccase [60] and later also by Fet3p [65], on the basis inter alia of spectral evidence similar to that described above (see below).

Spectroscopic studies combined with theoretical calculations have been undertaken for *R. vernicifera* laccase and most recently the yeast ferroxidase Fet3p, where the reaction of O_2 with the reduced, yet modified, enzymes was examined. The peroxide intermediate, apparently identical with the *R. vernicifera* peroxylaccase described above, was trapped by adding O_2 to the reduced, T1 mutated or T1(Hg)

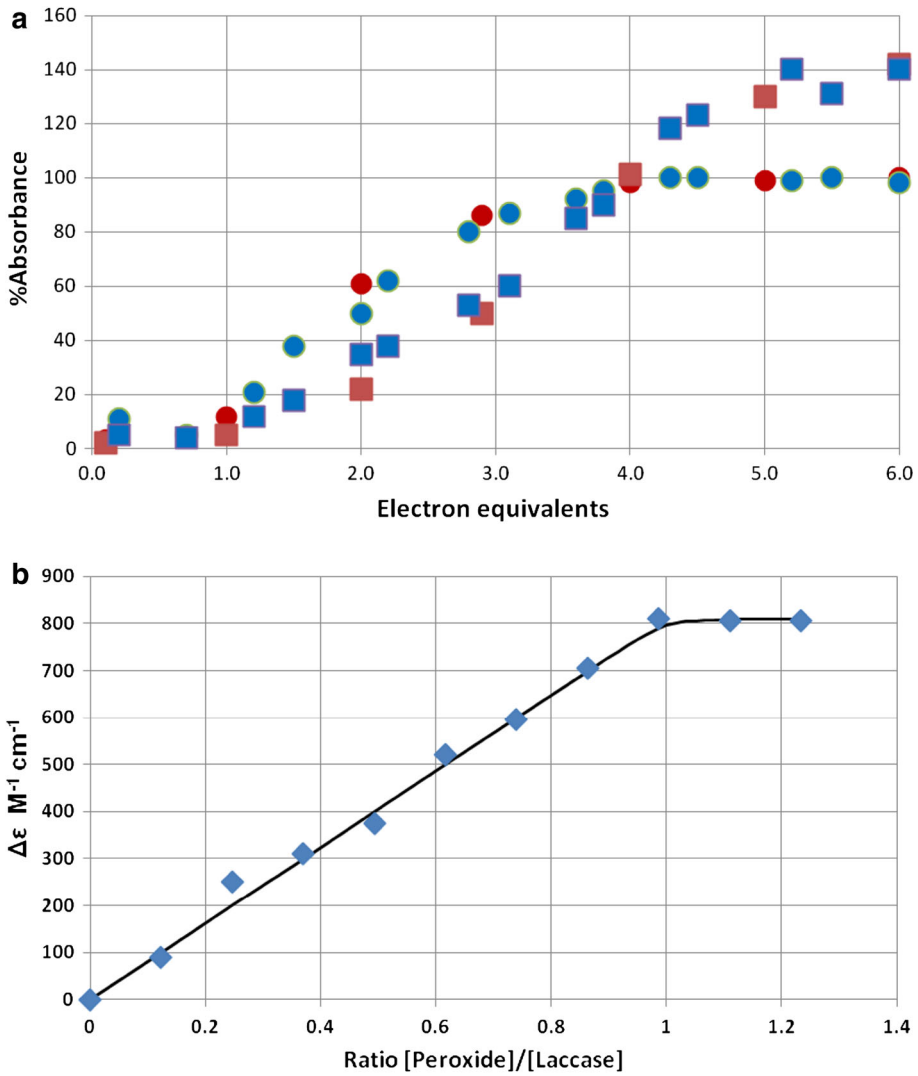

Fig. 6 **a** Redox titrations of *R. vernicifera* laccase. To a 0.20 mM laccase solution, an equimolar amount of H_2O_2 was added and the mixture was left overnight with a trace amount of either catalase or platinum black in order to remove free peroxide. After argon saturation, the laccase solution was reductively titrated with ascorbate (*red symbols*). When full reduction had been achieved, the laccase solution was titrated with H_2O_2 (*blue symbols*). *Circles* represent T1 site (615 nm) and *squares* represent T3 site (325 nm) absorption. The absorption values were calculated as $(A - A_{red})/(A_{ox} - A_{red})$ in percent, where A is the measured absorbance corrected for dilution, and A_{ox} and A_{red} are the absorbances of the fully oxidized and fully reduced chromophore, respectively; 100 % represents fully oxidized laccase, and 140 % represents absorbance of the peroxylaccase complex. **b** Titration of oxidized *R. vernicifera* laccase with hydrogen peroxide. To a 3.0 μM laccase solution, small aliquots of 1.0 mM H_2O_2 were added. $\Delta\varepsilon_{325}$ was calculated as the extinction difference between peroxide-treated and fully oxidized laccase, corrected for dilution. The curve was calculated using $K = 1 \times 10^9$ M^{-1}. (From [55])

derivative, i.e., to a three-electron-containing enzyme [62, 65, 66]. The structural model proposed has the peroxide interacting with all three TNC copper ions, with one oxygen atom bridging the T3 copper ions and the other oxygen atom bridging one of the T3 copper ions and the T2 copper ion (or a slightly different structure supported by calculations) [48, 67]. Thus, the current model of peroxide formation in the initial two-electron reduction step of O_2 is widely accepted, although details of the ET to the TNC as well as the role of the T2 site do differ [68]. A very recent communication addressed the issue of O_2 reduction intermediates, also in the context of a long-standing issue of the so-called pulsed and as isolated enzyme forms [68]. The latter form clearly has a slower catalytic cycle and has been observed for several but not all MCOs. This raises the question of what changes these enzyme forms require to attain full activity. In the work reported in [68], the reduction kinetics of wild-type *R. vernicifera* laccase in the absence of oxygen, in its so-called native intermediate and resting forms, were investigated by stopped-flow

spectrophotometry, following reaction of fully reduced laccase with O_2. Interestingly, although different terminology was used to describe the observed enzymatic states, the results are essentially identical with those obtained more than three decades earlier [57]. Namely, a long-lived intermediate with distinct spectroscopic features was identified, Further, the different possible pathways of *R. vernicifera* laccase cycles were addressed by examining in detail the reactivity of fully and partially reduced laccase with O_2, as well as reductively titrating peroxylaccase or oxidizing the fully reduced enzyme with hydrogen peroxide.

Although a peroxide intermediate is expected to be a common feature of the oxidation half-cycle of all MCOs, its stability and the conditions under which it forms are apparently variable. Oxidized AO was also shown to form the peroxide complex when the oxidized enzyme was titrated with hydrogen peroxide, as demonstrated by the appearance of the characteristic absorption change of the 325-nm band [69]. Moreover, the 3D structure of the AO–peroxy complex, produced by soaking the crystals in 10 mM hydrogen peroxide solution for 2 h, has also been determined, using a conventional X-ray source [15]. However, efforts to produce similar peroxide complexes from CotA and SLAC (our unpublished results) have failed, at least insofar as producing an intermediate absorbing at 330 nm on their reaction with hydrogen peroxide.

Important insights into the potential steps of O_2 reduction have evolved in recent years through the use of synchrotron radiation for 3D structure determination of different redox enzymes, MCOs included. The radiation-induced reduction of redox centers, in the presence of oxygen, has led to the production and identification of different MCO-bound O_2 reduction intermediates, usually formed under conditions of limited, gradually increased reduction as illustrated by the following examples. Structures showing enzyme-bound peroxide have been reported for CotA laccase [70] as well as for laccases isolated from *Lentinus tigrinus* [71] and *Pycnoporus cinnabarinus* [72]. In the radiation-dose-dependence study of *S. ochraceum* laccase discussed in "Structure of the TNC in MCOs" [12], a peroxide intermediate representing 20 % reduction was observed in the structure. The O_2 is coordinated to the T3 copper ions, but unlike the case of the 10 % reduced structure described in the section "Structure of the TNC in MCOs," it is now attached with one oxygen atom closer to one T3 copper ion and the other oxygen atom closer to the second T3 copper ion. The O–O distance has increased to 1.5 Å, typical for an O–O single bond, and the Cu–Cu distance has increased to 4.0 Å.

The step(s) in the oxidative catalytic half-cycle following the peroxide formation is(are) far less resolved and may also differ in details among MCOs. In the pioneering studies of reduced *R. vernicifera* laccase oxidation using ^{17}O-labeled O_2, the suggestion was made that a single electron reduction step causes breaking of the O–O bond of the peroxide intermediate and produces an ^{17}O free radical intermediate identified by EPR [54]. It was assigned to a copper-bound O^- radical which decays in parallel to the reappearance of an oxidized T2 copper with a half-life of approximately 13 s. This notion is in line with later results obtained by the use of ^{18}O-labeled O_2 showing that only one water molecule (produced as a result of a three-electron reduction) is released immediately into the bulk solvent. The second water molecule is produced only on transfer of the fourth electron to the T2-copper-bound radical, and remains bound for a relatively prolonged time [52, 59].

The evidence suggesting a role for the T2 copper site in the O_2 reduction led to an examination of the NMR line width of T2 Cu(II) in ^{17}O-enriched water, further illustrating the ligand interactions of the T2 site and the model where interaction with oxygen atoms involves the entire TNC [73].

Another model based almost entirely on results of 3D MCO structures suggests concomitant two-electron transfer to the bound peroxide, causing O–O bond cleavage and product protonation, followed by the formation of a hydroxide bridge between the two T3 copper ions and migration of the second oxygen atom to ligate the T2 copper ion [71].

Significantly, a recent report [74] yielded the first clear evidence for marked differences among MCOs in the final steps of the peroxide reduction. Both EPR and optical spectroscopy were used to investigate the products of O_2 reduction by SLAC. Both wild-type and a T1 copper mutated SLAC derivative were shown to produce a free radical, probably derived from the Tyr108 side chain, in the reaction of the reduced enzyme with O_2. Use of additional SLAC mutants, where Tyr108 had been replaced by phenylalanine or alanine, established the latter assignment of the Tyr108 radical, exchange-coupled with the unpaired spin of the T2 Cu(II). This further suggested that of the four electrons required for the formation of two water molecules, one is provided from the latter transient free radical. Since the trimeric, two-domain SLAC structure differs from the structures of most of the laccases studied so far, and also exhibits a distinct pattern of the internal ET rate and distribution dependence on the reduction state of the enzyme (vide supra), it remains to be learned if the above-mentioned distinct intermediate formed is a singularity or a characteristic of the trimeric two-domain MCO subfamily.

Candidate structures for a state of the enzyme in which the O–O bond is broken (called the "native" intermediate) have also been provided by spectroscopic and theoretical

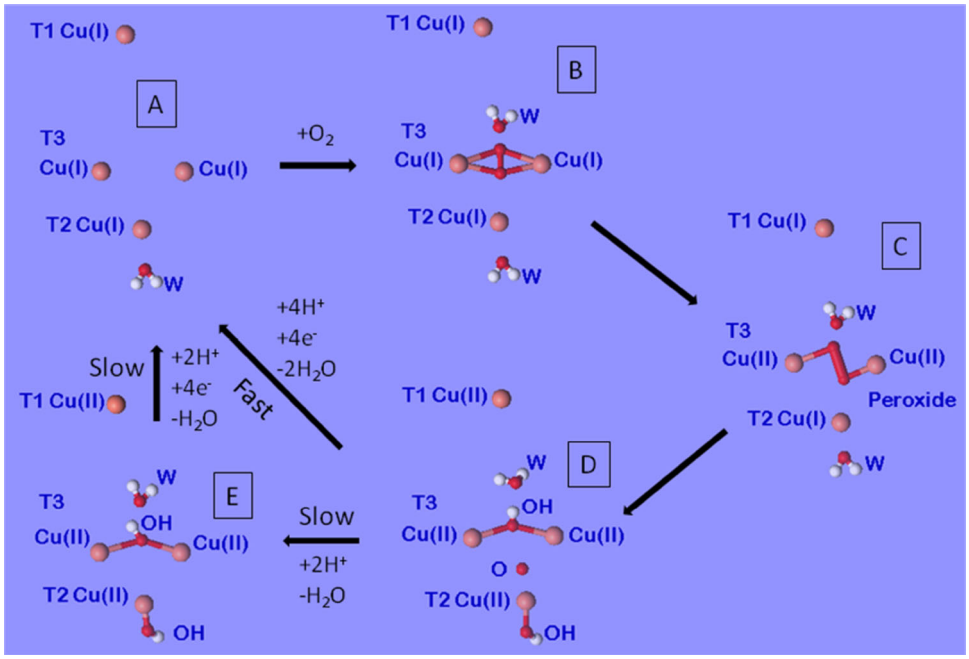

Fig. 7 The catalytic mechanism of multicopper oxidases based on the intermediates observed in the structural study of laccase from *Lentinus tigrinus* (Protein Data Bank code 2QT6) by Ferraroni et al. [71]. The reduced enzyme (*A*) reacts with molecular oxygen (*B*) to generate the peroxide intermediate (*C*). The peroxide bridges only the T3 copper pair and is not connected to the reduced T2 copper center. The peroxide intermediate is further reduced in a second step, oxidizing the T2 center and the distant T1 center to generate the "native intermediate" (*D*), which is composed by one μ^3-oxo bridge between the T2/T3 copper centers of the trinuclear cluster and an OH^- bridge between the two T3 copper ions. The resting oxidized enzyme (*E*) acts too slowly to be consistent with the catalytic turnover rate. The "native intermediate" (*D*) is catalytically active and is rapidly reduced by substrate. *W* water (Reproduced from [71] with kind permission of the authors)

studies of *R. vernicifera* laccase and Fet3p as well as from X-ray crystal structure determinations. The structure proposed from the spectroscopic measurements [48, 65] is based on the oxidation by O_2 of three-electron-reduced mutants lacking the T1 site. An oxide ion is proposed to be bound at the center of the triangle of Cu(II) ions and a hydroxide that bridges the T3 copper ions. The series of structures of *S. ochraceum* laccase produced through reduction by synchrotron radiation shows a similar structure produced after 60 % reduction. The two oxygen atoms (oxide or hydroxide ions, the protonation state could not be established directly) have separated to approximately 3 Å and the Cu–Cu distance is 4.8–5.0 Å.

A mechanism that is most consistent with the observations presented here and the series of X-ray crystal structures of *L. tigrinus* laccase is illustrated in Fig. 7 [71]. It assumes that O_2 only interacts with a TNC that already contains one or more reduction equivalents. In the former case, a superoxide is produced. This is in line with our results showing that a T1 copper to T3 copper ET equilibrium is established in several MCOs on uptake of the first single reduction equivalent. It may allow O_2 binding even as a superoxide, although no direct evidence is available. On an additional single-electron transfer to the T3 Cu(II), the peroxide would be formed. The involvement of the T2 copper in the latter intermediate is possible, although this model has neither thermodynamic nor kinetic evidence. As detailed already, in the pioneering studies of *R. vernicifera* laccase by Aasa et al. [54], the T2 site has been proposed to be implicated in the reductive bond fission of O_2. This is supported by the structures suggested for the "native" intermediate with an oxide ion from O_2 bridging to the T2 copper. In view of the differences observed in activity between different MCOs between "as isolated" and "cycled" (or "pulsed") samples, the consensus is that the resting enzyme is not part of the catalytic cycle. The state of the enzyme that is longest-lived under steady-state conditions may depend on the concentration of the reducing substrate and O_2 and the probability that the enzyme forms the resting state as opposed to continuing being in the activated enzyme loop. It is expected that this, in turn, will depend on the source of the enzyme and the conditions, especially the oxygen level, for which it is adapted.

Conclusion

We can answer the different questions raised in this review as follows. The internal T1 copper to T3 copper ET rate, although differeing considerably among MCOs, is markedly

enhanced in the presence of O_2 or on formation of O_2 reduction intermediates. In the absence of this terminal acceptor, so far only one MCO, SLAC of *S. coelicolor*, has shown a clear ET rate dependence on the degree of the T3 copper reduction, a pattern possibly indicating adaptation to limited substrate availability. One structural rationale for the change in the internal ET rate is based on possible changes in the TNC structure induced on electron uptake. Several interesting structures of O_2 reduction intermediates have been resolved by the 3D structure determined by the use of synchrotron radiation that are likely to be related to kinetic intermediates, peroxylaccase in particular. Different chemical and physical methods have provided evidence for additional intermediary states of the enzymes, some being a result of limited reduction equivalents, but possibly also distinct structural features of MCO family members. A particular characteristic of MCOs is the striking difference in activity, notably in their internal ET rates, when examined in the freshly isolated form and after participation in catalysis. The structural basis of this difference is still unclear, although it probably stems from the TNC.

One especially important conclusion has emerged from the kinetic studies of different MCOs. Namely, although representing a coupled system, the T3 site does take up single electrons as evidenced by the changes in its absorption band occurring synchronously with disappearance of the T1 site band.

A general concluding note regarding the many mechanistic schemes proposed so far is that attention needs to be given to the nature of the intermediates produced under different degrees of MCO reduction that occur under the various physiological conditions to which the wide diversity of MCOs may be exposed.

Acknowledgment O.F. thanks the Kimmelman Center for Biomolecular Structure and Assembly at the Weizmann Institute of Science for generous support.

References

1. Reiss R, Ihssen J, Richter M, Eichhorn E, Schilling B, Thony-Meyer L (2013) PLoS ONE 8:e65633. doi:10.1371/journal.pone.0065633
2. Messerschmidt A (1993) In: Karlin K, Tyeklar Z (eds) Bioinorganic chemistry of copper. Chapman & Hall, New York, pp 471–484
3. Farver O, Tepper AWJW, Wherland S, Canters GW, Pecht I (2009) J Am Chem Soc 131:18226–18227. doi:10.1021/ja908793d
4. Skalova T, Dohnalek J, Ostergaard LH, Osteryaard PR, Kolenko P, Duskova J, Stepankova A, Hasek J (2009) J Mol Biol 385:1165–1178. doi:10.1016/j.jmb.2008.11.024
5. Komori H, Miyazaki K, Higuchi Y (2009) FEBS Lett 583:1189–1195. doi:10.1016/j.febslet.2009.03.008
6. Lawton TJ, Sayavedra-Soto LA, Arp DJ, Rosenzweig AC (2009) J Biol Chem 284:10174–10180. doi:10.1074/jbc.M900179200
7. Lindley PF, Card G, Zaitseva I, Zaitsev V, Reinhammar B, Selin-Lindgren E, Yoshida K (1997) J Biol Inorg Chem 2:454–463. doi:10.1007/s007750050156
8. Nakamura K, Go N (2005) Cell Mol Life Sci 62:2050–2066. doi:10.1007/s00018-004-5076-5
9. Rydén LG, Hunt LT (1993) J Mol Evol 36:41–66. doi:10.1007/bf02407305
10. Liu B, Chen Y, Doukov T, Soltis SM, Stout CD, Fee JA (2009) Biochemistry 48:820–826. doi:10.1021/bi801759a
11. Enguita FJ, Marcal D, Martins LO, Grenha R, Henriques AO, Lindley PF, Carrondo MA (2004) J Biol Chem 279:23472–23476. doi:10.1074/jbc.M314000200
12. Ferraroni M, Matera I, Chernykh A, Kolomytseva M, Golovleva LA, Scozzafava A, Briganti F (2012) J Inorg Biochem 111:203–209. doi:10.1016/j.jinorgbio.2012.01.011
13. Messerschmidt A, Rossi A, Ladenstein R, Huber R, Bolognesi M, Gatti G, Marchesini A, Petruzzelli R, Finazziagro A (1989) J Mol Biol 206:513–529. doi:10.1016/0022-2836(89)90498-1
14. Messerschmidt A, Ladenstein R, Huber R, Bolognesi M, Avigliano L, Petruzzelli R, Rossi A, Finazziagro A (1992) J Mol Biol 224:179–205. doi:10.1016/0022-2836(92)90583-6
15. Messerschmidt A, Luecke H, Huber R (1993) J Mol Biol 230:997–1014. doi:10.1006/jmbi.1993.1215
16. Solomon EI, Szilagyi RK, George SD, Basumallick L (2004) Chem Rev 104:419–458. doi:10.1021/cr0206317
17. Climent V, Zhang JD, Friis EP, Ostergaard LH, Ulstrup J (2012) J Phys Chem C 116:1232–1243. doi:10.1021/jp2086285
18. Messerschmidt A, Huber R (1990) Eur J Biochem 187:341–352. doi:10.1111/j.1432-1033.1990.tb15311.x
19. Onuchic JN, Beratan DN, Winkler JR, Gray HB (1992) Annu Rev Biophys Biomol Struct 21:349–377
20. Meyer TE, Marchesini A, Cusanovich MA, Tollin G (1991) Biochemistry 30:4619–4623. doi:10.1021/bi00232a037
21. Andréasson L-E, Reinhammar B (1979) Biochim Biophys Acta 568:145–156. doi:10.1016/0005-2744(79)90282-1
22. Marcus RA, Sutin N (1985) Biochim Biophys Acta 811:265–322. doi:10.1016/0304-4173(85)90014-x
23. Gray HB, Winkler JR (2003) Q Rev Biophys 36:341–372. doi:10.1017/s0033583503003913
24. Farver O, Wherland S, Koroleva O, Loginov DS, Pecht I (2011) FEBS J 278:3463–3471. doi:10.1111/j.1742-4658.2011.08268.x
25. Farver O, Pecht I (1991) Mol Cryst Liq Cryst 194:215–224. doi:10.1080/00268949108041167
26. Farver O, Bendahl L, Skov LK, Pecht I (1999) J Biol Chem 274:26135–26140. doi:10.1074/jbc.274.37.26135
27. Farver O, Pecht I (1992) Proc Natl Acad Sci USA 89:8283–8287. doi:10.1073/pnas.89.17.8283
28. Farver O, Wherland S, Pecht I (1994) J Biol Chem 269:22933–22936
29. Shleev S, Christenson A, Serezhenkov V, Burbaev D, Yaropolov A, Gorton L, Ruzgas T (2005) Biochem J 385:745–754
30. Shleev SV, Morozova O, Nikitina O, Gorshina ES, Rusinova T, Serezhenkov VA, Burbaev DS, Gazaryan IG, Yaropolov AI (2004) Biochimie 86:693–703. doi:10.1016/j.biochi.2004.08.005
31. Tepper A, Aartsma TJ, Canters GW (2011) Faraday Discuss 148:161–171. doi:10.1039/c002585bc
32. Reinhammar B (1972) Biochim Biophys Acta 275:245–259. doi:10.1016/0005-2728(72)90045-x
33. Frasconi M, Favero G, Boer H, Koivula A, Mazzei F (2010) Biochim Biophys Acta 1804:899–908. doi:10.1016/j.bbapap.2009.12.018
34. Faraggi M, Pecht I (1973) J Biol Chem 248:3146–3149
35. Machczynski MC, Vijgenboom E, Samyn B, Canters GW (2004) Protein Sci 13:2388–2397. doi:10.1110/ps.04759104

36. Beratan DN, Skourtis SS, Balabin IA, Balaeff A, Keinan S, Venkatramani R, Xiao D (2009) Acc Chem Res 42:1669–1678. doi:10.1021/ar900123t
37. Li HT, Chang TN, Chang WC, Chen CJ, Liu MY, Gui LL, Zhang JP, An XM, Chang WR (2005) Biochem Biophys Res Commun 338:1935–1942. doi:10.1016/j.bbrc.2005.09.199
38. Farver O, Goldberg M, Pecht I (1980) Eur J Biochem 104:71–77. doi:10.1111/j.1432-1033.1980.tb04401.x
39. Kyritsis P, Messerschmidt A, Huber R, Salmon GA, Sykes AG (1993) J Chem Soc Dalton Trans 731–735. doi:10.1039/dt9930000731
40. Kroneck PMH, Armstrong FA, Merkle H, Marchesini A (1982) Adv Chem Ser 200:223–248
41. Nakamura T, Makino N, Ogura Y (1968) J Biochem (Tokyo) 64:189–195
42. Kataoka K, Sugiyama R, Hirota S, Inoue M, Urata K, Minagawa Y, Seo D, Sakurai T (2009) J Biol Chem 284:14405–14413. doi:10.1074/jbc.M808468200
43. Quintanar L, Stoj C, Wang TP, Kosman DJ, Solomon EJ (2005) Biochemistry 44:6081–6091. doi:10.1021/bi047379c
44. Silva CS, Damas JM, Chen Z, Brissos V, Martins LO, Soares CM, Lindley PF, Bento I (2012) Acta Crystallogr Sect D Biol Crystallogr 68:186–193. doi:10.1107/s0907444911054503
45. Bento I, Silva CS, Chen Z, Martins LO, Lindley PF, Soares CM (2010) BMC Struct Biol 10. doi:10.1186/1472-6807-10-28
46. Farver O, Pecht I (2011) Coord Chem Rev 255:757–773. doi:10.1016/j.ccr.2010.08.005
47. Kosman DJ (2010) J Biol Inorg Chem 15:15–28. doi:10.1007/s00775-009-0590-9
48. Rulisek L, Ryde U (2013) Coord Chem Rev 257:445–458. doi:10.1016/j.ccr.2012.04.019
49. Tepper AWJW, Milikisyants S, Sottini S, Vijgenboom E, Groenen EJJ, Canters GW (2009) J Am Chem Soc 131:11680. doi:10.1021/ja900751c
50. Taylor AB, Stoj CS, Ziegler L, Kosman DJ, Hart PJ (2005) Proc Natl Acad Sci USA 102:15459–15464. doi:10.1073/pnas.0506227102
51. Andreasson LE, Brändén R, Reinhammar B (1976) Biochim Biophys Acta 438:370–379. doi:10.1016/0005-2744(76)90254-0
52. Brändén R, Deinum J, Coleman M (1978) FEBS Lett 89:180–182. doi:10.1016/0014-5793(78)80550-x
53. Aasa R, Brändén R, Deinum J, Malmström BG, Reinhammar B, Vänngård T (1976) FEBS Lett 61:115–119. doi:10.1016/0014-5793(76)81016-2
54. Aasa R, Brändén R, Deinum J, Malmström BG, Reinhammar B, Vänngård T (1976) Biochem Biophys Res Commun 70:1204–1209. doi:10.1016/0006-291x(76)91030-5
55. Farver O, Goldberg M, Lancet D, Pecht I (1976) Biochem Biophys Res Commun 73:494–500. doi:10.1016/0006-291x(76)90734-8
56. Farver O, Goldberg M, Pecht I (1978) FEBS Lett 94:383–386. doi:10.1016/0014-5793(78)80983-1
57. Goldberg M, Farver O, Pecht I (1980) J Biol Chem 255:7353–7361
58. Farver O, Frank P, Pecht I (1982) Biochem Biophys Res Commun 108:273–278. doi:10.1016/0006-291x(82)91862-9
59. Brändén R, Deinum J (1977) FEBS Lett 73:144–146. doi:10.1016/0014-5793(77)80967-8
60. Sundaram UM, Zhang HH, Hedman B, Hodgson KO, Solomon EI (1997) J Am Chem Soc 119:12525–12540. doi:10.1021/ja972039i
61. Brissos V, Chen ZJ, Martins LO (2012) Dalton Trans 41:6247–6255. doi:10.1039/c2dt12067d
62. Augustine AJ, Kjaergaard C, Qayyum M, Ziegler L, Kosman DJ, Hodgson KO, Hedman B, Solomon EI (2010) J Am Chem Soc 132:6057–6067. doi:10.1021/ja909143d
63. Kau LS, Spira-Solomon DJ, Penner-Hahn JE, Hodgson KO, Solomon EI (1987) J Am Chem Soc 109:6433–6442. doi:10.1021/ja00255a032
64. Farver O, Pecht I (1979) FEBS Lett 108:436–438
65. Kjaergaard CH, Qayyum MF, Augustine AJ, Ziegler L, Kosman DJ, Hodgson KO, Hedman B, Solomon EI (2013) Biochemistry 52:3702–3711. doi:10.1021/bi4002826
66. Palmer AE, Quintanar L, Severance S, Wang TP, Kosman DJ, Solomon EI (2002) Biochemistry 41:6438–6448. doi:10.1021/bi011979j
67. Chalupsky J, Neese F, Solomon EI, Ryde U, Rulisek L (2006) Inorg Chem 45:11051–11059. doi:10.1021/ic0619512
68. David E, Heppner DE, Kjaergaard CH, Solomon EI (2013) J Am Chem Soc 135:12212–12215. doi:10.1021/ja4064525
69. Marchesini A, Kroneck PMH (1979) Eur J Biochem 101:65–76. doi:10.1111/j.1432-1033.1979.tb04217.x
70. Bento I, Martins LO, Lopes GG, Carrondo MA, Lindley PF (2005) Dalton Trans 3507–3513. doi:10.1039/b504806k
71. Ferraroni M, Myasoedova NM, Schmatchenko V, Leontievsky AA, Golovleva LA, Scozzafava A, Briganti F (2007) BMC Struct Biol 7:60. doi:10.1186/1472-6807-7-60
72. Antorini M, Herpoël-Gimbert I, Choinowski T, Sigoillot J-C, Asther M, Winterhalter K, Piontek K (2002) Biochim Biophys Acta 1594:109–114. doi:10.1016/S0167-4838(01)00289-8
73. Goldberg M, Vuk Pavlovic S, Pecht I (1980) Biochemistry 19:5181–5189. doi:10.1021/bi00564a005
74. Gupta A, Nederlof I, Sottini S, Tepper AWJW, Groenen EJJ, Thomassen EAJ, Canters GW (2012) J Am Chem Soc 134:18213–18216. doi:10.1021/ja3088604